Mechanical Systems and Signal Processing 25 (2011) 1431–1450

Contents lists available at ScienceDirect

Mechanical Systems and Signal Processing

journal homepage: www.elsevier.com/locate/jnlabr/ymssp

Tutorial Review

# Explaining operational modal analysis with data from an arch bridge

Filipe Magalhães, Álvaro Cunha *

*University of Porto, Faculty of Engineering (FEUP), R. Dr. Roberto Frias, 4200-465 Porto, Portugal*

ARTICLE INFO

*Article history:*
Received 3 August 2010
Accepted 6 August 2010

ABSTRACT

This tutorial paper aims to introduce the topic of operational modal analysis to non-specialists on the subject. First of all, it is stressed the relevance of this experimental technique particularly in the assessment of important civil infrastructure. Then, after a synthesis of required theoretical background, three of the most powerful algorithms for output-only modal identification are presented. The several steps of these identification procedures are illustrated with the processing of data collected on a concrete arch bridge with a span of 280 m. As the use of operational modal analysis in the context of structural health monitoring is a subject under active research, this theme is also introduced and briefly exemplified with data continuously recorded at the same bridge.



**Contents**



* Corresponding author. Tel.: +351 22 508 1580; fax: +351 22 508 1835
*E-mail address:* acunha@fe.up.pt (Á. Cunha).
*URL:* http://www.fe.up.pt/vibest (Á. Cunha).

0888-3270/$ - see front matter © 2010 Elsevier Ltd. All rights reserved.
doi:10.1016/j.ymssp.2010.08.001

## 1. Introduction

Experimental identification of modal parameters is a research topic with more than six decades of history. It started to be applied in Mechanical Engineering to characterize the dynamic behaviour of relatively small structures tested in a controlled environment, inside a laboratory. This first approach, nowadays called experimental modal analysis (EMA), is based on the performance of forced vibration tests (FVT), involving the simultaneous measurement of one or more dynamic excitations and the corresponding structural response. From the relation between the applied input and the observed output, it is possible to accurately identify modal parameters. Since the first practical applications until now, the testing equipment and the algorithms for data processing have evolved significantly. Therefore, EMA is currently a well-established field founded on solid theoretical bases extensively documented in reference books [1–3] and largely used in practice, particularly in aerospace and automotive industries. Several relevant applications are documented in the issues of the Mechanical System and Signal Processing Journal (MSSP) published during the last 25 years and in the proceedings of the International Modal Analysis Conference (IMAC), an annual conference organized since 1982.

EMA techniques can also be adopted for identification of modal parameters of Civil Engineering structures, like bridges, dams or buildings. Though, their large size imposes additional challenges. In particular, the application of controlled and measurable dynamic excitations requires the use of very heavy and expensive devices [4].

Therefore, in the case of Civil Engineering structures, ambient vibration tests (AVT) are much more practical and economical, since the artificial excitation produced by heavy shakers is replaced by freely available ambient forces, like the wind or the traffic circulating over or nearby the structure under analysis. As a consequence, AVT have the very relevant advantage of permitting the dynamic assessment of important civil infrastructure, like bridges, without disturbing their normal operation. Furthermore, as structures are characterized using real operation conditions, in case of existence of non-linear behaviour, the obtained results are associated with realistic levels of vibration and not with artificially generated vibrations, as it is the case when FVT are used.

Also in Mechanical Engineering, operational modal analysis proved to be very useful: for instance to obtain the modal parameters of a car during road testing or of an airplane during flight tests.

Nevertheless, as the level of excitation is low, very sensitive sensors with very low noise levels have to be used and even so, one should expect much lower signal to noise ratios than the ones observed in traditional tests. Besides this, AVT have two additional disadvantages when compared to FVT: the frequency content of the excitation may not cover the whole frequency band of interest, especially in the case of very stiff structures with high natural frequencies, and modal masses are not estimated, or mode shapes are not scaled in absolute sense, unless additional tests with extra masses over the structure are performed [5].

As with ambient vibration tests the modal information is derived from structural responses (outputs) while the structure is in operation, this identification process is usually called operational modal analysis (OMA) or output-only modal analysis (in opposition to input–output modal analysis). As the knowledge of the input is replaced by the assumption that the input is a realization of a stochastic process (white noise), the determination of a model that fits the measured data is also named stochastic system identification.

The modal properties provided by the application of operational modal analysis are useful to check, and if necessary update, numerical models of new structures, to tune vibration control devices that might have been adopted, to evaluate the safety of existing structures in the context of inspection programs, to characterize existent structures before the development of rehabilitation projects or to obtain a base-line characterization of an existent structure that may be used in the future as reference to check the evolution of its dynamic characteristics.

The large increase of research activity around the theoretical basis of OMA and its applications has motivated the creation, in 2005, of the International Operational Modal Analysis Conference (IOMAC) and also the recent edition of a special issue of the MSSP Journal [6].

The present paper aims to provide an overview of the theoretical background behind operational modal analysis and describe the steps needed for the identification of modal parameters from experimental data. Despite the existence of a large number of alternative OMA algorithms developed during the last decades, they are however just based on few basic principles. Therefore, this work is exclusively focused on the description of three methods with completely distinct theoretical backgrounds, which have also proven to provide very accurate estimates in civil engineering applications: frequency domain decomposition (FDD), covariance driven stochastic subspace identification (SSI-COV) and poly-least squares complex frequency domain (p-LSCF). The main operations of the algorithms are illustrated with the processing of data collected in a concrete arch bridge.

Therefore, this work starts with a brief description of the full-scale structure used to illustrate the application of the OMA techniques. Then, the presentation of basic theoretical background is followed by the description of the identification algorithms. Afterwards, it is provided an introduction to automated modal analysis, a topic under active research due to its importance in the context of vibration-based structural health monitoring. Finally, the conclusions also indicate some additional references especially dedicated to practical applications of operational modal analysis, for broadening and deepening of the readers' knowledge.

## 2. Description of the application

The presentation of the algorithms for operational modal analysis is going to be illustrated with the processing of datasets collected at the Infante D. Henrique Bridge, a long span concrete arch bridge located in the city of Porto, in Portugal (Fig. 1).

This bridge is composed of two fundamental elements: a very rigid prestressed reinforced concrete box girder, 4.50 m deep, supported by an extremely shallow and thin reinforced concrete arch, 1.50 m thick, as shown in the elevation represented in Fig. 2. The arch spans 280 m between abutments and rises 25 m until the crown. In the 70 m central segment, arch and deck meet to define a box-beam 6 m deep. The arch has constant thickness and its width increases linearly from 10 m in the central span up to 20 m at the springs [7].

This bridge is equipped with a dynamic monitoring system that comprises 12 acceleration channels, which have been programmed to continuously acquire the bridge response to ambient excitation [8]. The accelerometers are distributed in the four sections of the bridge deck marked in Fig. 2. Each section is instrumented with three accelerometers: two to measure the vertical accelerations at the lateral edges of the deck (characterizing vertical movements and rotations) and another one to measure lateral accelerations. The system was configured to acquire acceleration signals with a sampling frequency of 50 Hz and produce time segments with a length of 30 min.

In order to illustrate the application of the identification algorithms described in the next section, the dataset collected at 23:00 of 22/10/2007 was adopted. For didactic purposes, instead of using the 12 collected time series, the identification was just based on the four time series presented in Fig. 3: the average of the two vertical acceleration time series measured in each instrumented section. The reduction of the amount of data to be processed permits to include more details in the explanation of the identification techniques.

**Fig. 1.** View of Infante D. Henrique Bridge from downstream (Porto at the left side).

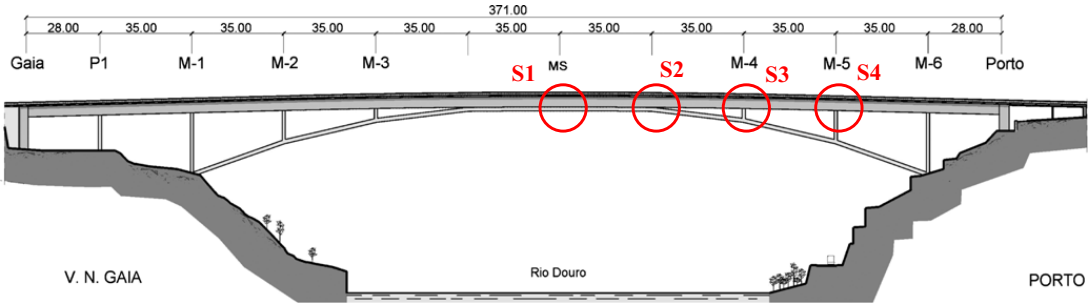


**Fig. 2.** Elevation of the bridge showing the instrumented sections: S1–S4.

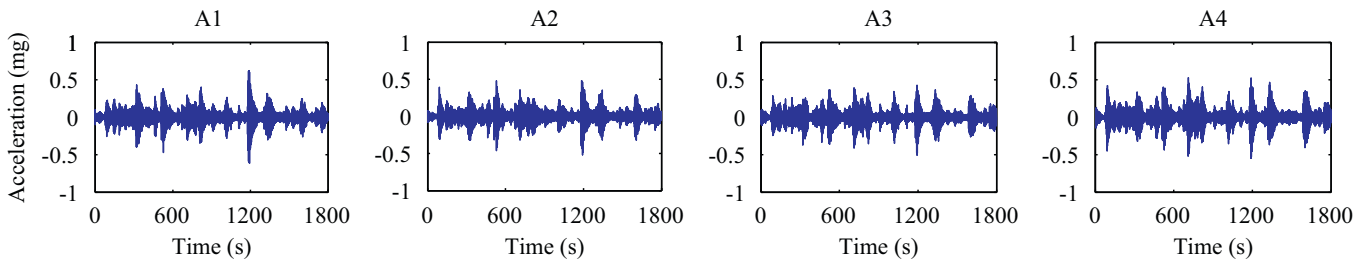


**Fig. 3.** Average vertical acceleration time series.

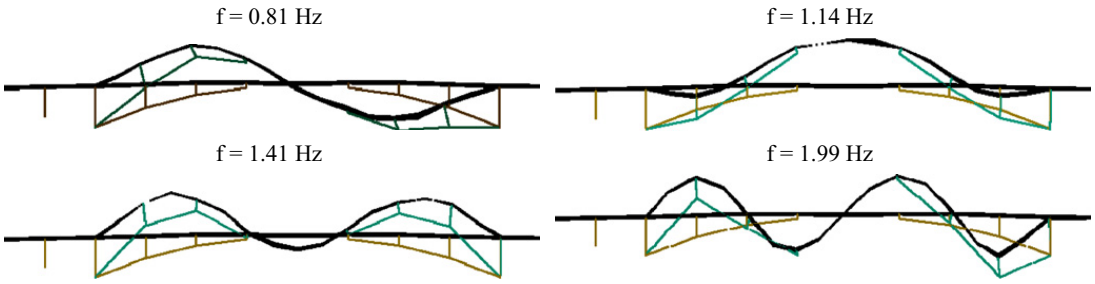


**Fig. 4.** First four identified vertical bending modes.

As a consequence, the obtained results are restricted to the first four vertical bending modes, only characterized by four modal components. The achieved estimates can be compared with the ones presented in Fig. 4, which were obtained with a very complete ambient vibration test, described in [8].

## 3. Theoretical background

The identification of modal parameters is usually performed with the purpose of obtaining accurate experimental estimates of natural frequencies, mode shapes and modal damping ratios, which can be then correlated with the corresponding values numerically estimated from a finite element model of the structure under analysis [9].

The majority of the modal identification methods are based on models (called experimental models) of the tested dynamic system that are fitted to the recorded data and from which it is then possible to extract estimates of modal parameters. This section is devoted to the characterization of some alternative experimental models that can be derived from the finite element model.

This subject has already been extensively explored in some reference books [1,10]. So, only the essential concepts needed for the understanding of the identification methods described in this paper are presented here. Therefore, emphasis will be given to models that assume an unknown or stochastic input, as these are the ones used for operational modal analysis.

### 3.1. Finite element model

The analysis of a complex dynamic system requires its previous discretization through the construction of a finite element model with a finite number of degrees of freedom ($n_2$). After this first step, the equilibrium of such system is represented by the following differential equation expressed in matrix form:

$$M\ddot{q}(t)+C_1\dot{q}(t)+Kq(t)=p(t)=B_2u(t) \tag{1}$$

where $M$, $C_1$, $K \in \mathrm{R}^{n_2\times n_2}$ are the mass, damping and stiffness matrices; $\ddot{q}(t)$, $\dot{q}(t)$, $q(t)$ are time functions organized in column vectors that characterize the evolution of the acceleration, velocity and displacement of each degree of freedom (each dot over a time function denotes one derivation with respect to time) and $p(t)$ is a column vector with the forces applied to the system. As normally not all the degrees of freedom (*dof*) are excited, the load vector with $n_2$ lines can be replaced by a vector of inferior dimension ($n_i < n_2$) containing the time evolution of the $n_i$ applied inputs. This vector, designated by $u(t)$, is multiplied by a matrix that maps the $n_i$ inputs with the $n_2$ *dof* of the system: $B_2$, a $n_2$-by-$n_i$ matrix composed by ones and zeros.

### 3.2. Stochastic state-space model

The previous second-order system of differential equations can be transformed into a first-order one, the state equation, using simple mathematical manipulations [10]. A state-space model is obtained by combining the state equation with the observation equation:

$$\begin{aligned}\dot{x}(t)&=A_Cx(t)+B_Cu(t)\\ y(t)&=C_Cx(t)+D_Cu(t)\end{aligned} \tag{2}$$

where $A_C$, designated state matrix, is a $n$-by-$n$ matrix, with $n$ equal to $2n_2$, and $x(t)$ is the state vector, which contains the displacements and the velocities vectors of the dynamic system. The observation equation establishes a relation between a subset of $n_o$ measured outputs organized in vector $y(t)$ and the $n_i$ inputs of dynamic system $u(t)$. $C_C$ is the output matrix and $D_C$ is designated direct transmission matrix [10].

The modal parameters of the dynamic system can be extracted from the state matrix $A_C$. In [11] it is demonstrated that the matrices with the eigenvalues and eigenvectors of $A_C$ ($\Lambda_C$ and $\Psi$, respectively) have the following structure:

$$A_C=\Psi\Lambda_C\Psi^{-1}$$

$$\Lambda_C = \begin{bmatrix} \Lambda & 0 \\ 0 & \Lambda^* \end{bmatrix}, \quad \Psi = \begin{bmatrix} \Theta & \Theta^* \\ \Theta\Lambda & \Theta^*\Lambda^* \end{bmatrix}$$
$$\Lambda = \begin{bmatrix} \ddots & & \\ & \lambda_k & \\ & & \ddots \end{bmatrix}, \quad \Theta = \begin{bmatrix} \cdots & \phi_k & \cdots \end{bmatrix}, \quad k = 1,\ldots,n_2 \tag{3}$$

where $\bullet^*$ means complex conjugate. The $\lambda_k$ are related with the structure frequencies ($\omega_k$—natural frequencies in rad/s) and modal damping ratios ($\xi_k$) by the expression:

$$\lambda_k = -\xi_k\omega_k + i\sqrt{1-{\xi_k}^2}\,\omega_k \tag{4}$$

where $i = \sqrt{-1}$.

The mode shapes are represented in Eq. (3) by $\phi_k$. However, as only a subset of the *dof* is measured, the observable modal components are given by

$$\Phi = C_C\Psi \tag{5}$$

The number of modes ($n_m$) is equal to the dimension of the finite element model ($n_2$) from which the state-space model was derived and equal to one half the dimension of the state-space model: $n_m = n/2$ ($n$, dimension of the state vector).

In a dynamic test, the analog signals recorded by the transducers are converted to digital data by an analog to digital converter (A/D), so that they can be stored and processed by a computer. Therefore, in practice, the available information of the dynamic system under study is discrete in time. Consequently, a discrete time version of the previously presented model is more adequate to fit experimental data. Furthermore, in the context of operational modal analysis, the system input is unknown. Therefore, the terms of the state-space model in $u(t)$ have to be represented by stochastic components:

$$\begin{aligned} x_{k+1} &= Ax_k + w_k \\ y_k &= Cx_k + v_k \end{aligned} \tag{6}$$

This model is designated discrete-time stochastic state-space model. The time functions $x(t)$ and $y(t)$ are replaced by their values at discrete time instants $k\,\Delta t$, where $k$ is an integer and $\Delta t$ is the adopted sampling interval: $x_k = x(k\Delta t)$. The vectors $w_k$ and $v_k$ model not only the effect of the unknown outputs, but also the noise due to disturbances and modelling inaccuracies, and the measurement noise due to sensor inaccuracy, respectively. Both vector signals with dimension $n$ are assumed to be zero mean realizations of stochastic processes with the following correlation matrices:

$$E\left(\begin{bmatrix} w_p \\ v_p \end{bmatrix}\begin{bmatrix} {w_p}^T & {v_p}^T \end{bmatrix}\right) = \begin{bmatrix} Q & S \\ S^T & R \end{bmatrix}$$
$$E\left(\begin{bmatrix} w_p \\ v_p \end{bmatrix}\begin{bmatrix} {w_q}^T & {v_q}^T \end{bmatrix}\right) = 0, \quad p \neq q \tag{7}$$

where the indexes $p$ and $q$ represent generic time instants and $E(\bullet)$ is the expected value of $\bullet$. As the correlations matrices of the processes $w_k$ and $v_k$, $E\left(w_p w_q^T\right)$ and $E\left(w_p w_q^T\right)$, are assumed to be equal to zero for any time delay $\tau = q - p$ different from zero, each new observation of these processes is independent from the previous ones. Such purely random stochastic processes are designated white noise processes.

In [10] the expressions that relate the discrete-time model matrices with their continuous-time counterparts are derived. There, it is also demonstrated that the eigenvectors of matrix $A$ coincide with the ones of matrix $A_C$. The eigenvalues of the discrete model, represented by $\mu_k$, are related with the ones of the continuous model $\lambda_k$ by the following equation:

$$\mu_k = e^{\lambda_k \Delta t} \Leftrightarrow \lambda_k = \frac{\ln(\mu_k)}{\Delta t} \tag{8}$$

Consequently, it is proven that once a discrete-time state-space model has been identified from experimental data, it is possible to estimate the modal parameters of the tested structure. The natural frequencies and model damping ratios are obtained from the eigenvalues of $A$ using Eqs. (8) and (4). Taking into account that $C$ is equal to $C_C$ and that the eigenvectors of $A$ coincide with the eigenvectors of $A_C$, the observable modal components are given by Eq. (5).

Stochastic state-space models present several properties that are essential for the justification of the identification algorithms presented later. These are described and proven in [12]. The most important property is the following relation between the correlation matrix of the measured structural responses and the state-space matrix:

$$R_j = CA^{j-1}\mathrm{G} \tag{9}$$

$R_j$ is the correlation matrix of the outputs for any arbitrary time lag $\tau = j\,\Delta t$ and $G$ is the "next state-output" correlation matrix defined as

$$G = E\left[x_{k+1}{y_k}^T\right] \tag{10}$$

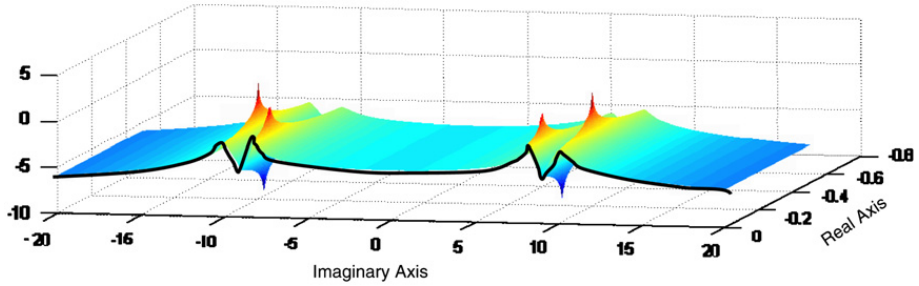


**Fig. 5.** Absolute value of the element (1,1) of the transfer function of a dynamic system with two degrees of freedom (vertical axis in logarithmic scale).

### 3.3. Transfer function

The application of the Laplace transform to the second-order differential equation of equilibrium (1), assuming zero initial conditions, leads to the following algebraic equation:

$$Ms^2Q(s)+C_1sQ(s)+KQ(s)=P(s)$$

or

$$\left[Ms^2+C_1s+K\right]Q(s)=P(s)\Leftrightarrow$$
$$Z(s)Q(s)=P(s) \tag{11}$$

where $Z(s)$ is designated dynamic stiffness matrix.

Therefore, it is possible to relate the Laplace transform of the outputs $Q(s)$ with the Laplace transform of the inputs $P(s)$ through a matrix called transfer function:

$$Q(s)=H(s)P(s)$$
$$H(s)=Z(s)^{-1}=\left[Ms^2+C_1s+K\right]^{-1} \tag{12}$$

Each element of the transfer function matrix is a complex valued function and therefore, it can be graphically represented by two surfaces defined in the Laplace or s-plane ($x$ axis—$\sigma$; $y$-axis—$i\omega$): the real and the imaginary parts or the absolute value and the phase angle. Fig. 5 shows the absolute value of the element (1,1) of the transfer function matrix of a dynamic system with two degrees of freedom. At the observed peaks, the amplitude of the transfer function is equal to infinite (the figure was constructed with a finite resolution and consequently the peaks present finite values). The values of $s$ in which the elements of the transfer function matrix present infinite values are designated poles.

The poles, represented by $\lambda_k$, are complex numbers whose real and imaginary components are related with the natural frequencies and modal damping ratios of the dynamic system by equation:

$$\lambda_k=-\xi_k\omega_k+i\sqrt{1-\xi_k{}^2}\omega_k$$

The real part depends on the natural frequency and on the modal damping ratio, whereas the imaginary part coincides with the damped natural frequency ($\sqrt{1-\xi_k{}^2}\omega_k$), which is close to the natural frequency when damping is small. As can be observed in Fig. 5, the poles appear in complex conjugate pairs. The expression for the poles coincides with the one presented for the eigenvalues of the continuous-time state-space model (Eq. (4)).

The matrix of frequency response functions (FRF) is composed by the cross sections of the elements of the transfer function matrix along the imaginary axis: $s=i\omega$. In the presented plot of the transfer function (Fig. 5), the absolute value of the corresponding FRF element is marked with a black line. Consequently, the FRF is simply a particular case of the transfer function. However, in practice, it may replace the transfer function with no loss of useful information [2]. The FRF function elements present peaks with finite amplitude (for damped structures) when $\omega$ is equal to the system damped natural frequencies and with a bell shape that becomes sharper when the damping decreases.

### 3.4. Modal model

The transfer function defined in Eq. (12), or equivalently the frequency response function (substituting $s$ by $i\omega$), can be expressed by the sum of the contributions of the dynamic system modes [2]:

$$H(s)=V(sI-\Lambda)^{-1}L^T=\sum_{k=1}^{n_2}\frac{\phi_k\gamma_k^T}{s-\lambda_k}+\frac{\phi_k^*\gamma_k^H}{s-\lambda_k^*}$$

$$\text{with} \quad \begin{matrix} V=\begin{bmatrix}\phi_1 & \cdots & \phi_{n_2} & \phi_1{}^* & \cdots & \phi_{n_2}^*\end{bmatrix} \\ L=\begin{bmatrix}\gamma_1 & \cdots & \gamma_{n_2} & \gamma_1^* & \cdots & \gamma_{n_2}^*\end{bmatrix} \end{matrix} \quad \Lambda=\begin{bmatrix}\lambda_1 & & & & & \\ & \ddots & & 0 & & \\ & & \lambda_{n_2} & & & \\ & & & \lambda_1^* & & \\ & 0 & & & \ddots & \\ & & & & & \lambda_{n_2}^*\end{bmatrix} \tag{13}$$

where $n_2$ is the number of modes, $\bullet^*$ is the complex conjugate of a matrix or vector, $\bullet^H$ is the complex conjugate transpose of a matrix or vector, $I$ is a $2n_2$-by-$2n_2$ identity matrix, $\phi_k$ is a column vector containing the $n_2$ components of mode shape $k$, $\gamma_k^T$is a line vector with the $n_2$ components of the modal participation factor of mode $k$ and $\lambda_k$, for $k=1,\ldots, n_2$, are the structure poles.

A transfer function more close to the experimental world should only relate the *dof* where the inputs are applied with the measured outputs, and so it is a $n_i$-by-$n_o$ matrix instead of a $n_2$-by-$n_2$ matrix. In addition, not all the modes are observable and so the summation is limited to a subset of modes.

### 3.5. Right matrix fraction model

The modal model is the model in the frequency (or Laplace) domain that provides the best physical understanding from an engineering point of view. However, it is not adequate to be directly fitted to experimental data, as it is highly non-linear. Matrix fraction models (fully described in [13]) are more abstract models that can be more easily fitted to measured data and then used to obtain estimates of modal parameters.

In particular, the Right Matrix Fraction Model defines the Transfer Function as the right division (B/A) of two polynomial matrices:

$$\begin{aligned} &H(s)=B(A)^{-1} \\ &H(s)=\left[\sum_{r=0}^{p_b} B_r s^r\right]\left[\sum_{r=0}^{p_a} A_r s^r\right]^{-1} \end{aligned} \tag{14}$$

where the matrices $B_r$ are $n_o$-by-$n_i$ and the matrices $A_r$ are $n_i$-by-$n_i$. $p_a$ and $p_b$ are the orders of the denominator and numerator polynomials.

Once the model matrices have been estimated, the natural frequencies and the modal damping ratios can be extracted from the coefficients of the denominator polynomial and the mode shapes determined from the coefficients of $B$. Instead, it is also possible to convert the estimated right matrix-fraction model into a state-space model (Eq. (2)). The equations needed to make this transposition have been derived in [14], assuming $p_a=p_b=p$ and that the degree of the polynomial with the determinant of $A(s)$ is equal to $p\cdot n_i$:

$$\begin{aligned} A_C &= \begin{bmatrix} -A_p^{-1}A_{p-1} & -A_p^{-1}A_{p-2} & \ldots & -A_p^{-1}A_1 & -A_p^{-1}A_0 \\ I & 0 & \ldots & 0 & 0 \\ \vdots & \ddots & \ldots & \vdots & \vdots \\ 0 & 0 & \ldots & I & 0 \end{bmatrix} \\ B_C &= \begin{bmatrix} A_p^{-1} \\ 0 \end{bmatrix} \\ C_C &= \begin{bmatrix} B_{p-1}-B_pA_p^{-1}A_{p-1} & \ldots & B_0-B_pA_p^{-1}A_0 \end{bmatrix} \\ D_C &= B_pA_p^{-1} \end{aligned} \tag{15}$$

After this step, the modal parameters can be estimated from the state-space model matrices, following the procedure presented in the previous sub-section. As the $A_C$ matrix is a square matrix with dimension $pn_i$, the model represents a dynamic system with $pn_i/2$ modes.

### 3.6. Output spectrum and half-spectrum

In the context of Operational Modal Analysis, the stochastic process used to represent the unknown inputs can be characterized either by a correlation matrix (as in Eq. (7)) or by a matrix with the input spectra (Laplace transforms of the input correlations).

The output spectrum matrix $S_{yy}$, restricted to $s=i\omega$, is related with the input spectrum matrix $S_{uu}$ by the following equation [15]:

$$S_{yy}(\omega)=H(\omega)S_{uu}(\omega)H^H(\omega) \tag{16}$$

In the particular case where the input is assumed to be a white noise, the output spectrum only depends on the system transfer function $H(\omega)$ and on a constant matrix that coincides with the white noise input correlation matrix:

$$S_{yy}(\omega) = H(\omega) R_{uu} H^H(\omega) \tag{17}$$

Taking into account the modal decomposition of the transfer function (Eq. (13)), it is also possible to express the output spectrum as a superposition of the contribution of the structure modes. Considering the contribution of all the system modes ($n_2$), the following equation is obtained [11]:

$$S_{yy}(\omega) = \sum_{k=1}^{n_2} \frac{\phi_k g_k^T}{i\omega - \lambda_k} + \frac{\phi_k^* g_k^H}{i\omega - \lambda_k^*} + \frac{g_k \phi_k^T}{-i\omega - \lambda_k} + \frac{g_k^* \phi_k^H}{-i\omega - \lambda_k^*} \tag{18}$$

where the vectors $g_k$, called operational reference vectors, take the place of the modal participation factors. However, these vectors do not depend only on the characteristics of mode $k$. As proven in [11], each $g_k$ depends on all the structure modal parameters, on the input locations and on the input correlation matrix.

The modal decomposition of the output spectrum shows that this has four poles ($\lambda_k$, $-\lambda_k$, $\lambda_k^*$ and $-\lambda_k^*$) for each mode. This imposes the use of models with orders that are twice the model order needed to model the transfer function of the same dynamic system. This disadvantage can be avoided by the use of the so-called positive or half-spectrum. It is demonstrated, for instance in [13], that the modal decomposition of the half-spectrum is given by

$$S_{yy}^+(\omega) = \sum_{k=1}^{n_2} \frac{\phi_k g_k^T}{i\omega - \lambda_k} + \frac{\phi_k^* g_k^H}{i\omega - \lambda_k^*} \tag{19}$$

As this equation has exactly the same structure as the modal decomposition of the transfer function, or of the frequency response function, all the previously described models can be also adopted to model half-spectrum matrices.

## 4. Modal parameters identification

### 4.1. Overview of OMA methods

The methods available to perform the identification of modal parameters of dynamic systems based on their response to ambient excitation are usually classified as frequency domain or time domain methods.

Frequency domain methods start from output spectrum or half-spectrum matrices previously estimated from the measured outputs, as described in Section 4.2. These methods can be either non-parametric or parametric. The non-parametric frequency domain methods are simpler and therefore were the first ones to be used [16]. Among these, the Peak-Picking method is the most well-known, being still widely applied nowadays in dynamic testing of civil engineering structures, as it is the most adequate method to make a first check of the quality of collected data and get a first insight into the system dynamic properties.

The frequency domain decomposition (FDD) is a slightly more sophisticated non-parametric frequency domain method that overcomes some of the limitations of the Peak–Picking method. This method is going to be described with some detail in Section 4.3.

Alternatively, the identification in the frequency domain can be based on the fitting of a model to the output spectrum or half-spectrum matrix, from which the modal parameters are extracted in a second phase. There are several models that can be used for such purpose: the modal model, the common-denominator model, the right and left matrix-fraction descriptions (two of these were described in the Section 3). The fitting of experimental data to a model is an optimization problem based on a cost function, which can be solved either through the linear least squares method or with the maximum likelihood (ML) estimator [17]. All the possible combinations of the previously referred models and fitting procedures are explored in [13], together with a different class of methods (realization algorithms) that use frequency domain state-space models, designated stochastic frequency-domain subspace identification methods. In [18], it is introduced an alternative frequency domain identification algorithm based on the concept of transmissibility functions. Still, it has to be said that most of the parametric frequency-domain methods for operational modal analysis stemmed from the transposition of algorithms previously developed for input–output modal analysis.

In the present paper, only one frequency domain parametric method is described with detail: the poly-least squares complex frequency domain method (p-LSCF). This was selected as it is the most commonly used in civil engineering applications among this class of methods. This is due to its good performance, but also to its implementation in a commercial software package (Test.Lab from LMS) under the name PolyMax.

The similarity between the mathematical expressions of the transfer function and of the output half-spectrum of a system excited by white noise, presented in Section 3.6, is in correspondence with the similarity, in the time domain, between the output correlations of a system excited by white noise and the impulse responses [19]. This was explored in the early ages of operational modal analysis based on time domain methods, in order to adapt the already existing techniques for the analysis of impulse responses recorded in the context of forced vibration tests. For instance, the well-known eigensystem realization algorithm (ERA) method [20] was converted to an OMA method, the NExT, by James et al. [21].

Nowadays, the available time domain methods for operational modal analysis, extensively explored in [11], are essentially based on two types of models: discrete-time stochastic state-space models and auto-regressive moving average (ARMA) or just auto-regressive (AR) models.

The formulations that use state-space models, designated stochastic subspace identification (SSI) methods, constitute the parametric approach that is more commonly adopted for civil engineering applications. The model can be identified either from correlations (or covariances) of the outputs: Covariance driven stochastic subspace identification—SSI-COV; or directly from time series collected at the tested structure by the use of projections [12]: data driven stochastic subspace identification—SSI-DATA. As reported in [11], these two methods are very closely related. Still, the SSI-COV has the advantage of being faster and based on simpler principles, whereas the SSI-DATA permits to obtain some further information with a convenient post-processing, as for instance, the decomposition of the measured response in modal contributions. In the present paper, only the algorithm of the SSI-COV method is explored.

On the other hand, methods based on ARMA or AR models, investigated in [22], are not so frequently used by the civil engineers community. ARMA models can be for instance identified from the output correlations using the Instrumental Variable (IV) method [11]. If the output correlations are substituted by impulse responses, the equations of this method coincide with the ones of a standard method for EMA: the Polyreference Time Domain (PTD) method. It is also possible to estimate ARMA or AR models directly from the output time signals using the least squares method. However, these approaches have not yet reached a level of robustness adequate for practical applications.

All the output-only modal identification methods assume that the ambient excitation, known to provide multiple inputs with wide band frequency content, is a zero mean white noise. As this assumption is not fully realistic, the true excitation can be considered as the output of a linear filter subjected to a white noise, which means that the identified modal parameters are not only associated with the tested structure but also with the imaginary system that produced the real excitation. Generally, in practice, it is possible to separate the modal parameters associated with the structural system from the others that may be due to the excitation, since it is known that the vibration modes of civil engineering structures have usually low damping and smooth mode shapes with real components.

### 4.2. Pre-processing

The identification methods presented in this section are based on discrete time series of measured accelerations. However, these time series have to be pre-processed before the application of the identification algorithms.

The parametric method in the time domain that is going to be presented requires a correlation matrix of the outputs. This is defined as

$$R_j = \lim_{n_t \to \infty} \frac{1}{n_t} \sum_{k=0}^{n_t-1} y_k y_{k+j}^T \tag{20}$$

In real applications the number of available samples ($n_t$) is not infinite and so an estimate of the correlation matrix is obtained by dropping the limit. The calculation of the correlation matrix with direct application of the previous formula is very time consuming. However, it is possible to obtain the same results using of a high-speed FFT-based approach, described in [23].

The methods in the frequency domain can be based either on output spectrum matrices or on output half-spectrum matrices.

The output spectrum matrix can be obtained following two classical alternative approaches for the estimation of the spectra between two outputs: the periodogram and the correlogram.

The Periodogram approach, also known as Welch estimator [24], calculates the spectra directly from the measured time series and involves the following steps. First, the response records are divided in $n_b$ segments $y_b$ with the same length ($n_{tb}$), which may present some percentage of overlap. Then, it is calculated the discrete Fourier transform (DFT) of each block after the application of a window $w_k$:

$$Y_b(\omega_j) = \sum_{k=0}^{n_{tb}-1} w_k y_{b,k} e^{-i\omega_j k \Delta t} \tag{21}$$

The window aims the minimization of leakage, an error expressed by the spreading of the true spectrum components along other neighbouring frequencies and motivated by the finite nature of the time segments [3]. Since the window reduces the contribution of the data at the beginning and end of each block, the adoption of some overlap between adjacent blocks is advisable. A Hanning window [3] is very commonly used together with an overlap of 50%.

Afterwards, the estimate of the output spectrum matrix, a $n_o$-by-$n_o$ matrix represented by $\hat{S}_{yy}(\omega_j)$, is the average of the spectra associated with the several data blocks, given by $Y_b(\omega_j)Y_b(\omega_j)^H$:

$$\hat{S}_{yy}(\omega_j) = \frac{1}{n_b} \sum_{b=1}^{n_b} Y_b(\omega_j) Y_b(\omega_j)^H \tag{22}$$

The selection of the length of each block and consequently the number of blocks is a trade-off between frequency resolution and irregularity of the spectra or, in other words, between bias and variance of the estimates. Selecting longer

blocks increases the resolution and reduces the effect of leakage, but the number of averages is smaller and thus the uncertainty is higher.

The Correlogram approach calculates the output spectrum from the DFT of the output correlation matrix:

$$S_{yy}(\omega_k) = \sum_{j=-\infty}^{+\infty} R_j e^{-i\omega_k j \Delta t} \tag{23}$$

If the DFT is extended to a limited number of both negative and positive time lags of the correlation function, a spectrum estimate is obtained; if the DFT is restricted to a limited number of positive time lags, a half-spectrum is estimated.

The evaluation of the DFT should be preceded by the application of a window to reduce the leakage. However, the application of this window influences the decay of the correlations and therefore has implications on the damping that is then estimated. Nevertheless, if an exponential window is used, the effect introduced by the window can be corrected later from the estimated modal damping ratios. Furthermore, this window also reduces the influence of noise in the tails of the correlations, where the correlation values are already very small.

### 4.3. FDD and EFDD

The so called Frequency Domain Decomposition method (FDD) was firstly presented by Brincker et al. [25]. However, the concepts behind the method had already been used in the analysis of structures subjected to ambient excitation by Prevosto [26] and Corrêa and Costa [27], and on the identification of modal parameters from FRF [28]. The method aims to be a simple and user-friendly technique allowing at the same time the separation of closely spaced modes and the identification of modal damping ratios. It is a frequency domain non-parametric method that interprets output spectrum matrices estimated with the Welch method.

According to the modal decomposition of the transfer function, presented in Eq. (13), and taking into account the relationship between the output spectrum and the transfer function (Eq. (17)), the following matrix expression for the output spectrum is obtained:

$$S_{yy}(\omega) = V(i\omega I - \Lambda)^{-1} L^T R_{uu} L^* (i\omega I - \Lambda)^{-1*} V^H \tag{24}$$

If it is assumed that the inputs are not correlated ($R_{uu}$ is a diagonal matrix) and that the mode shapes are orthogonal, and so the modal participation factors are also orthogonal, then the previous equation can be written as

$$S_{yy}(\omega) = VC(\omega)V^H \tag{25}$$

where $C(\omega)$ is a diagonal matrix composed by functions of $\omega$, each of them dependent on the natural frequency and modal damping ratio of only one mode of the structure, and $V$ is a matrix whose columns represent the mode shapes. The same simplification can be done even if the inputs are correlated, but the modal inputs ($L^T u(t)$) are uncorrelated. Moreover, if the structure is lightly damped, as it is the case of the majority of civil engineering structures, in the neighbourhood of the resonant frequencies, the simplification presented in eq. (25) is still approximately true even if there is some correlation between the inputs or the modal inputs, as it may occur if for instance the wind is the dominant excitation. However, the condition of orthogonality of the mode shapes has to be respected at least between closely spaced modes [25].

On other hand, the singular value decomposition (SVD) of the complete output spectrum matrix (a square Hermitian matrix, $S=S^H$) estimated from the measured signals gives

$$\hat{S}_{yy}(\omega_j) = U_j S_j U_j^H \tag{26}$$

where $U_j$ is a orthonormal matrix ($U_j U_j^H = I$) that contains the singular vectors of $\hat{S}_{yy}(\omega_j)$ and $S_j$ is a diagonal matrix holding the corresponding singular values.

The comparison between Eqs. (25) and (26) shows that the singular vectors provided by the SVD can be associated with the mode shapes of the tested structure and that the singular values are related with the ordinates of scalar spectra of single degree of freedom systems with the same modal parameters as the modes that contribute to the response of the multi-degree of freedom system under analysis. The singular value decomposition provides the singular values in ascending order, which means that for each discrete value of $\omega$, the first singular value contains an ordinate of the spectrum associated with the dominant mode at that frequency. The number of non-zero singular values represents the rank of the spectrum matrix at a specific frequency, or in other words, the number of modes with significant contribution to the system response at that particular frequency.

Fig. 6 presents, at the left side, the absolute values of the elements of the spectrum matrix calculated from the acceleration time series represented in Fig. 3. These were calculated with the Welch method using time segments with 4096 points, a Hanning window and an overlapping of 50%. The application of the SVD decomposition to the spectrum matrix evaluated at all the discrete frequencies between 0 and 2.5 Hz produces four singular values for each frequency. These are plotted in the upper right quadrant of Fig. 6. The spectrum of the first singular values presents four peaks that are associated with the four vertical bending modes of the bridge within the frequency band under analysis. The real components of first singular vectors associated with the identified peaks (first column of $U$ in Eq. (26)) are plotted in the

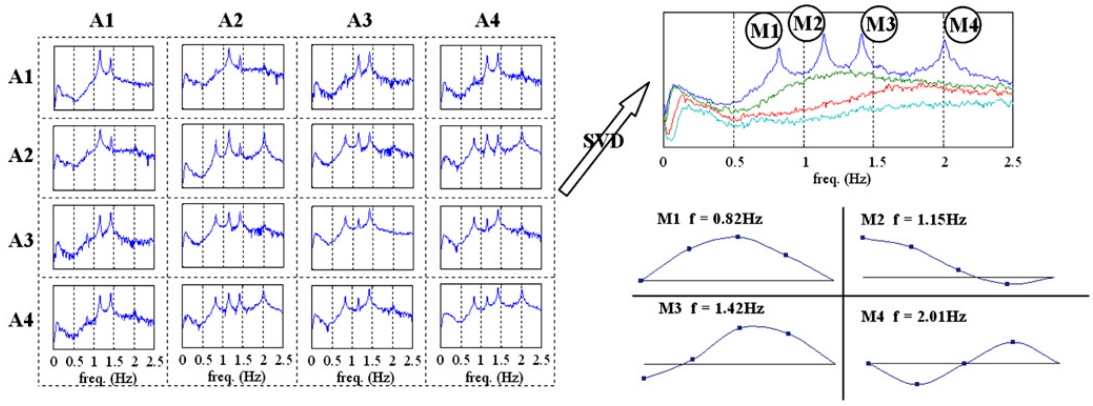


**Fig. 6.** FDD method, from the spectrum matrix to mode estimates.

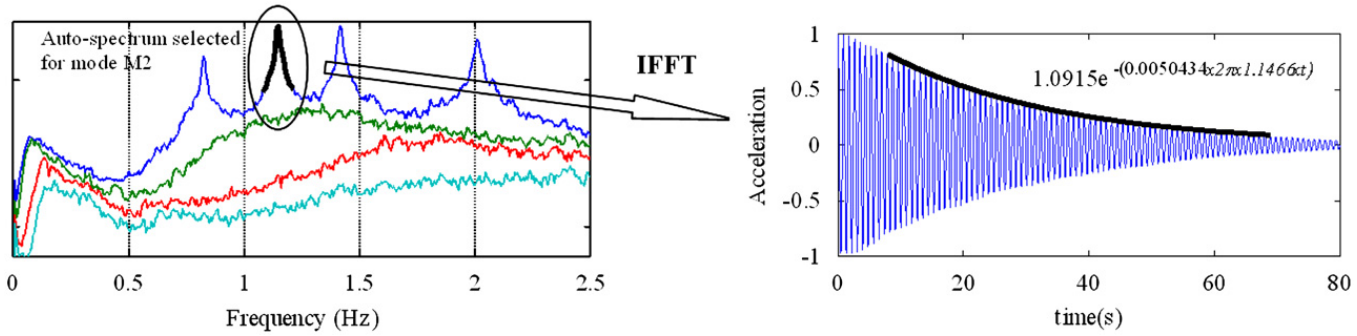


**Fig. 7.** FDD method, estimation of the modal damping ratio of the second mode.

bottom right quadrant of Fig. 6. These are good estimates of the components of the bridge first four vertical modes at the sections where the acceleration where measured. In fact, the obtained shapes coincide with the left half of the mode shapes presented in Fig. 4. The match between the estimated frequencies and the ones presented in Fig. 4 is not perfect, essentially due to the effect of ambient temperate on the structure stiffness (the ambient vibration test was performed during the summer while the setup under analysis was collected in October).

The points of the singular value spectra belonging to the spectra associated with each mode can be selected by comparing the singular vectors associated with the points in the vicinity of an identified resonant frequency with the singular vector associated with the peak that represents that frequency. This selection is usually performed establishing a limit for an index designated modal assurance criterion (MAC), which measures the correlation between two mode shapes ($\phi_1$, $\phi_2$) by the expression [29]:

$$MAC_{\phi_1,\phi_2} = \frac{\left(\phi_1^T \phi_2\right)^2}{\left(\phi_1^T \phi_1\right)\left(\phi_2^T \phi_2\right)} \tag{27}$$

This index varies from 1, when the modes only differ on a scale factor, to zero, when the modes are orthogonal.

In the left side of Fig. 7, the points of the singular value spectra represented in Fig. 6 associated with the second vertical bending mode of the bridge under analysis are selected, using a limit for the MAC of 0.8.

Once a set of points with similar singular vectors is selected for a given mode, this segment of an auto-spectrum may be converted to the time domain. An auto-correlation function with the contribution of a single mode is obtained. As the output correlation of a dynamic system excited by white noise is proportional to its impulse response, it is possible to estimate the modal damping ratio of the mode under analysis from the obtained correlation. This can simply be performed by fitting an exponential function to relative maxima of the correlation function and extracting the modal damping ratios from the parameters of the fitted expression taking into account the classical expression for the impulse response of a single degree of freedom [30]:

$$y(t) = a e^{-\xi_k 2\pi f_k t} \sin(2\pi f_k t) \tag{28}$$

where $a$ is a constant and $\xi_k$ and $f_k$ are the damping ratio and the natural frequency in Hz. Before the determination of the modal damping ratio, an enhanced estimate of the natural frequency may be obtained from the time intervals between zero crossings of the correlation function.

Such operation is illustrated in Fig. 7, where it is obtained an auto-correlation function from which it was possible to obtain an estimate for the modal damping ratio of the second bending mode: 0.50%. This operation can be repeated for other peaks to obtain estimates of the modal damping ratios of other modes.

The above described procedure to estimate modal damping ratios was firstly detailed in [31] under the name of Enhanced Frequency Domain Decomposition (EFDD) method. Other alternative implementations of the FDD/EFDD method are presented in [32–35].

### 4.4. SSI-COV

The Covariance driven Stochastic Subspace Identification method identifies a stochastic state-space model (Eq. (6)), from the output covariance matrix (or correlation, as the mean of the signals is assumed to be zero).

The starting point of this method is the output correlation matrix evaluated for positive time lags varying from 1 $\Delta t$ to $(2j_b-1)\,\Delta t$ represented by $R_1$ to $R_{2j_b-1}$ and organized in a $n_o j_b$-by-$n_o j_b$ block Toeplitz matrix ($n_o$—number of outputs):

$$T_{1|_{j_b}} = \begin{bmatrix} R_{j_b} & R_{j_b-1} & \cdots & R_1 \\ R_{j_b+1} & R_{j_b} & \cdots & R_2 \\ \cdots & \cdots & \cdots & \cdots \\ R_{2\cdot j_b-1} & R_{2\cdot j_b-2} & \cdots & R_{j_b} \end{bmatrix} \tag{29}$$

The correlation matrices used to describe the application of the SSI-COV method were calculated from the outputs presented in Section 2 after the application of a decimation that reduced the sampling frequency from 12.5 to 6.25 Hz (this is important to reduce the dimension of the matrices and so reduce the calculation effort). In the present analysis, these were evaluated for time lags ($j$ in Eq. (20)) between 1 and 29. The application of Eq. (29) to this particular case, adopting $j_b$=15, is illustrated in Fig. 8: the 29 4-by-4 correlation matrices are stored in a 60-by-60 Toeplitz matrix (a matrix in which each descending diagonal from left to right is constant).

If the factorization property of the correlation matrix presented in Eq. (9) is applied to all the $R_j$ matrices stored in the Toeplitz matrix, $T_{1|j_b}$ can be decomposed in the product of the following matrices:

$$T_{1|_{j_b}} = \begin{bmatrix} C \\ CA \\ \cdots \\ CA^{j_b-1} \end{bmatrix} \begin{bmatrix} A^{j_b-1}G & \ldots & AG & G \end{bmatrix} = O\Gamma \tag{30}$$

The second equality defines the matrices: $O$—extended observability matrix; and $\Gamma$—reversed extended stochastic controllability matrix. The first one is a column of $j_b$ blocks with dimensions $n_o$-by-$n$ ($n$ is the dimension of the state-space model). The second one is formed by $j_b$ $n$-by-$n_o$ matrices organized in a row. According to the previous equation, the Toeplitz matrix results from the product of a matrix with $n$ columns by a matrix with $n$ rows. Therefore, if $n < n_o\ j_b$, the rank of $T_{1|_{j_b}}$ is equal to $n$.

On the other hand, the singular value decomposition of the Toeplitz matrix yields:

$$T_{1|_{j_b}} = USV^T = \begin{bmatrix} U_1 & U_2 \end{bmatrix} \begin{bmatrix} S_1 & 0 \\ 0 & 0 \end{bmatrix} \begin{bmatrix} V_1^T \\ V_2^T \end{bmatrix} = U_1 S_1 V_1^T \tag{31}$$

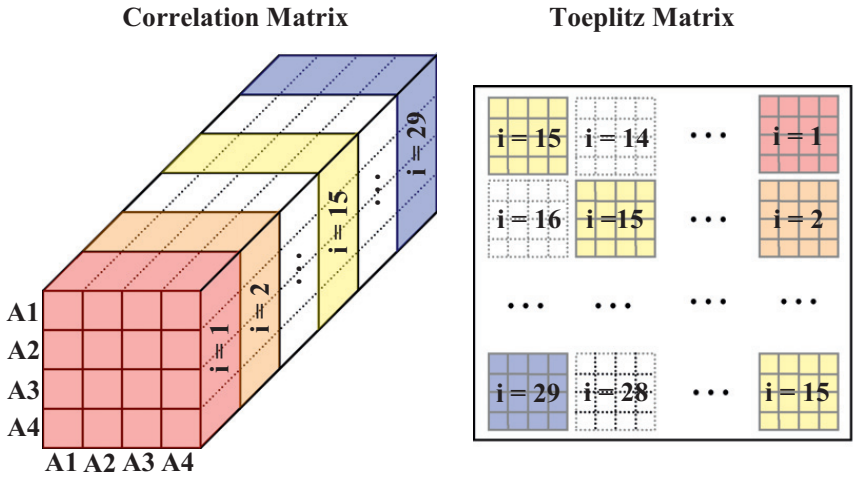


**Fig. 8.** Construction of the Toeplitz matrix.

The number of non-zero singular values gives the rank of the decomposed matrix, which, in this case, coincides with $n$ (assuming $n < n_o j_b$), the dimension of the state-space matrix $A$.

The comparison of Eqs. (30) and (31) shows that the observability and the controllability matrices can be calculated from the outputs of the SVD using, for instance, the following partition of the singular values matrix:

$$O = U_1 S_1^{1/2}$$
$$\Gamma = S_1^{1/2} V_1^T \tag{32}$$

There are alternative implementations of the SSI-COV method that pre and/or post multiply the Toeplitz matrix by weighting matrices before the SVD. These weighting matrices determine the state-space basis in which the model is identified. More details can be found in [12]. In the present work, it was used an implementation without weighting matrices.

Taking into account the structure of the observability and controllability matrices presented in Eq. (30), once these have been obtained, the identification of the state-space model matrices $A$ and $C$ is quite straightforward. Matrix $C$ can be extracted from the first $n_o$ lines of the observability matrix. The most efficient and robust procedure to obtain matrix $A$ is based on the shift structure of the observability matrix [36]. Thus, $A$ is the solution of a least squares problem expressed by the following equation:

$$\begin{bmatrix} C \\ CA \\ \dots \\ CA^{j_b-2} \end{bmatrix} A = \begin{bmatrix} CA \\ CA^2 \\ \dots \\ CA^{j_b-1} \end{bmatrix} \Leftrightarrow A = \begin{bmatrix} C \\ CA \\ \dots \\ CA^{j_b-2} \end{bmatrix}^{\dagger} \begin{bmatrix} CA \\ CA^2 \\ \dots \\ CA^{j_b-1} \end{bmatrix} = O^{to\dagger} O^{bo} \tag{33}$$

where $O^{to}$ contains the first $n_o(j_b-1)$ lines of $O$ and $O^{bo}$ contains the last $n_o(j_b-1)$ lines of $O_{j_b}$. The symbol $\bullet^{\dagger}$represents the Moore–Penrose pseudo-inverse of a matrix, which is used to solve least squares problems (minimizes the sum of the squared errors of the individual equations of an overdetermined system of equations) and that can be calculated, for instance, with the expression: $A^{\dagger} = (A^T A)^{-1} A^T$. Still, there are mathematical algorithms to calculate it in a more efficient way [37].

At this point, a state-space model that can represent the dynamics of the system under analysis has already been obtained. The modal parameters can be easily extracted from matrices $A$ and $C$. First, the eigenvalues of $A(\mu_k)$, which are the poles of the discrete-time state-space model, have to be related with the poles of the continuous-time model $\lambda_k$. Then, the poles with a positive imaginary component are used to obtain natural frequencies ($f_k$, in Hz) and modal damping ratios ($\xi_k$):

$$\lambda_k = \frac{\ln(\mu_k)}{\Delta t}$$
$$f_k = \frac{\mathrm{Abs}(\lambda_k)}{2\pi}$$
$$\xi_k = -\frac{\mathrm{Re}(\lambda_k)}{\mathrm{Abs}(\lambda_k)} \tag{34}$$

Abs($\bullet$) and Re($\bullet$) are the absolute value and the real part of the complex number $\bullet$.

The multiplication of matrix $C$ by the matrix with the eigenvectors of $A$ gives a $n_o$-by-$n$ matrix, which contain is its columns the observable components of the mode shapes. Due to the existence of complex conjugate pairs, only the columns associated with eigenvalues with positive imaginary components are selected. In this way, a state-space model of order $n$ provides modal parameters for $n/2$ modes.

In the context of practical applications, the method is based on estimates of the output correlation matrices, which are calculated from a limited number of samples. In addition to this, the tested structure may not have a perfect linear behaviour (modelling inaccuracies) and the collected signals are always contaminated by noise. Therefore, the derived state-space model matrices and the obtained modal parameters have to be considered also as estimates. Furthermore, the SVD of the Toeplitz matrix does not permit the identification of the model order, because the higher singular values that theoretically should be zero in practice present residual values. Current practice showed that using data collected in large structures, it is even not possible to identify any gap between consecutive singular values that would at least permit to obtain a reasonable estimate of the most adequate model order.

As a result, the most appropriate way to overcome this difficulty is to estimate models with orders within an interval previously fixed in a conservative way (the upper limit should be much higher than two times the number of physical modes of the system within the frequency range under analysis) and then, select the best model by the analysis of the corresponding modal parameters.

This can be accomplished in an efficient way, because the SVD of the Toeplitz matrix, the most demanding calculation, has only to be performed once. As long as the maximum model order, $n_x$, is defined, a Toeplitz matrix with at least $n_x/n_o$ blocks has to be constructed. Then, the SVD of the complete Toeplitz matrix is calculated. Models with successively decreasing orders are estimated by selecting a successively decreasing number of singular values and vectors for the calculation of the observability and controllability matrices.

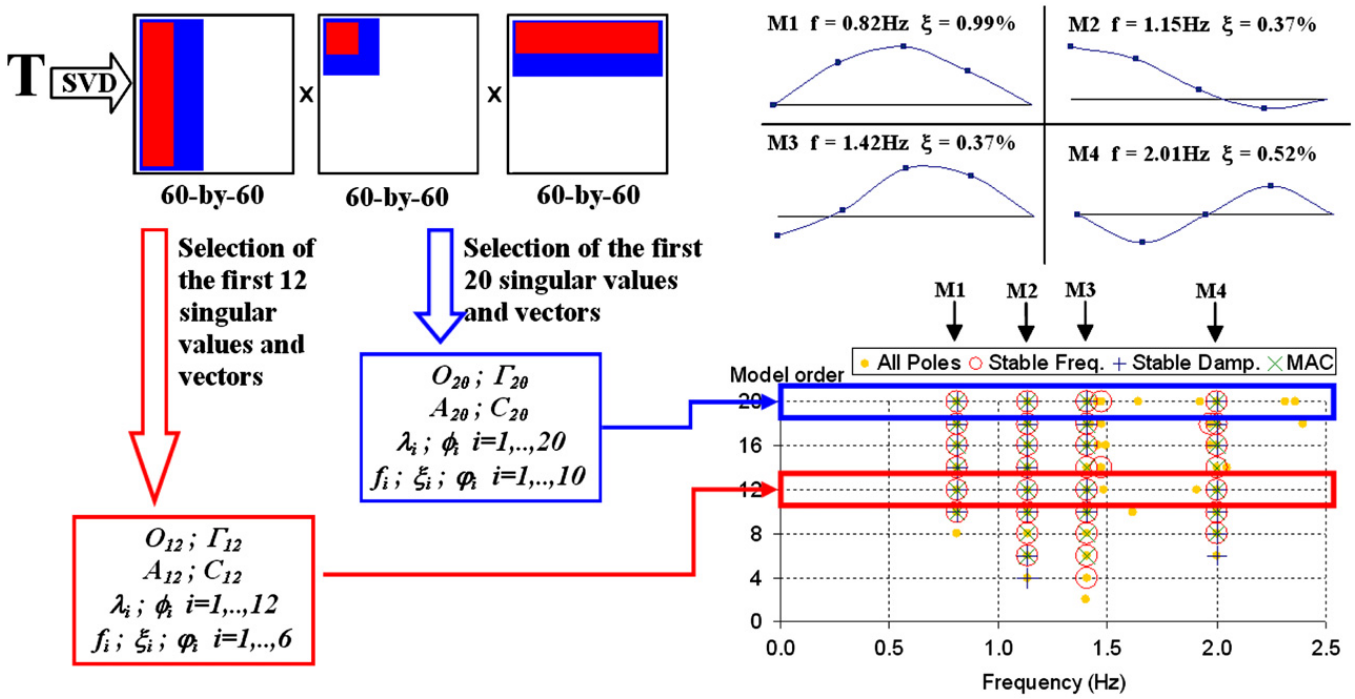


**Fig. 9.** SSI-COV method: from the Toeplitz matrix to stabilization diagrams and mode estimates.

However, the use of high model orders leads to the introduction of numerical modes (also called spurious or noise modes), which have little to none physical relevance but are needed to model the noise and to overcome the modelling inaccuracies.

Separation of physical and spurious modes is then a crucial step of the identification algorithm. The most popular approach to achieve that is based on the creation of stabilization diagrams. In these diagrams the modal parameter estimates provided by all the models are represented together ($x$-axis—natural frequency of the mode estimates; $y$-axis—order of the model), allowing the identification of the modal parameters that are stable for models of increasing orders. Modes that appear in most of these models with consistent frequency, mode shape and damping are classified as stable and are likely to be physical. Modes that only appear in some models are considered spurious.

The application of the SSI-COV method to the Toeplitz matrix calculated with the procedure presented in Fig. 8 is illustrated in Fig. 9. The application of the singular value decomposition to this 60-by-60 matrix produces three 60-by-60 matrices (Eq. (31)). Afterwards, matrices $O$, $\Gamma$, $A$ and $C$ and then the modal parameters are estimated considering an odd number of singular values and vectors varying from 2 to 20. In the figure, two cases are detailed: the selection of the first 12 singular values that leads to 6 mode estimates (extracted from a state-space model of order 12) and the selection of the first 20 singular values and vectors that produces 10 mode estimates. The mode estimates derived from the 10 adopted models are organized in the presented stabilization diagram. The estimates of consecutive model orders presenting similar natural frequencies, modal damping ratios and mode shapes are highlighted with different symbols (the meaning of the used symbols is described in the diagram). There are four vertical alignments of stable mode estimates that clearly stand out. These represent the four physical modes within the frequency range under analysis. In the same figure, the four mode estimates provided by model order 12 that belong to the vertical alignments of stable poles are also characterized. It can be observed that the selected estimates of natural frequencies and mode shapes are similar to the ones provided by the FDD method. In this case, the modal damping ratios are directly obtained from the model without any further post-processing.

With the goal of reducing the calculation effort of the SSI-COV algorithm, it is possible to slightly reformulate the SSI-COV method, so that it only needs the correlations between all outputs and a subset of selected outputs, designated references [38]. Moreover, in [39] it is presented an improved version of this method that provides confidence intervals for the obtained estimates of modal parameters.

### 4.5. *p-LSCF*

The polyreference Least Squares Complex Frequency Domain method (p-LSCF), also known by its commercial name PolyMAX (implemented in the software Test.Lab commercialized by LMS), is a recent parametric frequency domain method that was firstly developed to perform the identification of modal parameters from frequency response functions [40,41]. However, taking into account the similarities between the modal decomposition of the output half-spectrum of a system excited by white noise and its transfer function, or frequency response function (Eqs. (13) and (19)), the adjustment

of the method for operational modal analysis was quite straightforward. The output-only version of the method was firstly presented by Peeters and Van der Auweraer [42].

The method models the half-spectrum matrix using a right matrix-fraction model in the discrete-time frequency domain, the $z$-domain (the variable $s$ is replaced by $z=e^{s\Delta t}$). Therefore, considering the previously presented equation of this model (Eq. (14)), adopting polynomials of the same order for $B$ and $A$, and limiting $s$ to the imaginary axis ($s=i\omega$), the half-spectrum matrix evaluated at a given discrete frequency $\omega_j$ is modelled by

$$S_{yy}^{+}(\omega_j) = BA^{-1} = \left[\sum_{r=0}^{p} B_r\, e^{i\omega_j \Delta t r}\right]\left[\sum_{r=0}^{p} A_r\, e^{i\omega_j \Delta t r}\right]^{-1} \tag{35}$$

where $B_r$ and $A_r$ are matrices with the model parameters, $p$ is the order of the polynomials and $\Delta t$ is the sampling time used to measure the structural responses. The number of lines and columns of the half-spectrum is equal to the number of measured degrees of freedom ($n_o$). $B_r$ and $A_r$ are real-valued matrices with dimensions $n_o$-by-$n_o$.

The goal of the identification algorithm is to find the model parameters, matrices $B_r$ and $A_r$, that minimize the differences between the half-spectrum matrix estimated from the measured output time series (represented by $\hat{S}_{yy}^{+}$) and the theoretical half-spectrum matrix given by Eq. (35):

$$E^{NLS}(\omega_j) = \left[\sum_{r=0}^{p} B_r\, e^{i\omega_j \Delta t r}\right]\left[\sum_{r=0}^{p} A_r\, e^{i\omega_j \Delta t r}\right]^{-1} - \hat{S}_{yy}^{+}(\omega_j) \tag{36}$$

However, this equation for the error to be minimized leads to a non-linear least squares (NLS) problem. In order to avoid this extra complexity, and instead obtain a linear least squares problem, an alternative error equation is formulated by right multiplying the previous equation by $A$ [40], which gives

$$E^{LS}(\omega_j) = \left[\sum_{r=0}^{p} B_r\, e^{i\omega_j \Delta t r}\right] - \hat{S}_{yy}^{+}(\omega_j)\left[\sum_{r=0}^{p} A_r\, e^{i\omega_j \Delta t r}\right] \tag{37}$$

where $E^{LS}(\omega_j)$ is a $n_o$-by-$n_o$ matrix with the errors ($E_{o,r}$) to be minimized.

The model parameters can be determined using the least squares cost function, which is obtained by adding all the squared elements of the error matrix ($E_{o,r}$) evaluated at all the discrete frequency values, $\omega_1$ to $\omega_{n_f}$, within a previously selected frequency interval for the analysis:

$$\varepsilon = \sum_{o=1}^{n_o}\sum_{r=1}^{n_o}\sum_{j=1}^{n_f} E_{o,r}(\omega_j) E_{o,r}(\omega_j)^{*} \tag{38}$$

With some definitions this equation can be written in a more compact format. If the polynomial basis functions evaluated at $\omega_j$ are organized in one row vector with ($p$+1) components:

$$\boldsymbol{\Omega}(\omega_j) = \left[\begin{array}{cccc}\boldsymbol{\Omega}_0(\omega_j) & \boldsymbol{\Omega}_1(\omega_j) & \ldots & \boldsymbol{\Omega}_p(\omega_j)\end{array}\right] = \left[\begin{array}{cccc} e^{i\omega_j \Delta t 0} & e^{i\omega_j \Delta t 1} & \ldots & e^{i\omega_j \Delta t p}\end{array}\right] \tag{39}$$

Then, one general line $o$ of the error matrix can be calculated with the following equation (the subscript $^{LS}$ was dropped to simplify the notation):

$$E_o(\omega_j) = \boldsymbol{\Omega}(\omega_j)\cdot\begin{bmatrix} B_{0o} \\ B_{1o} \\ \vdots \\ B_{po}\end{bmatrix} + \left[\begin{array}{cccc}\boldsymbol{\Omega}_0(\omega_j)\hat{S}_{yyo}^{+} & \boldsymbol{\Omega}_1(\omega_j)\hat{S}_{yyo}^{+} & \ldots & \boldsymbol{\Omega}_p(\omega_j)\hat{S}_{yyo}^{+}\end{array}\right]\begin{bmatrix} A_0 \\ A_1 \\ \vdots \\ A_p\end{bmatrix} \tag{40}$$

where $B_{ro}$ represents the $o$ line of matrix $B_r$ and $\hat{S}_{yyo}^{+}$ represents the $o$ line of matrix $\hat{S}_{yy}^{+}$.

Introducing the following definitions:

$$\beta_o = \begin{bmatrix} B_{0o} \\ B_{1o} \\ \vdots \\ B_{po}\end{bmatrix} \text{ with } o = 1,2,\ldots,n_o \text{ and } \alpha = \begin{bmatrix} A_0 \\ A_1 \\ \vdots \\ A_p\end{bmatrix} \tag{41}$$

Eq. (40) can be generalized to all the discrete frequencies values, $\omega_1$ to $\omega_{n_f}$:

$$E_o(\beta_o,\alpha) = \left[\begin{array}{cc} X_o & Y_o\end{array}\right]\begin{bmatrix}\beta_o \\ \alpha\end{bmatrix}$$

with

$$X_o = \begin{bmatrix}\Omega(\omega_1) \\ \vdots \\ \Omega(\omega_{n_f})\end{bmatrix} \text{ for } o = 1,2,\ldots,n_o$$

$$Y_o = \begin{bmatrix} \Omega_0(\omega_1)\hat{S}^+_{yyo} & \Omega_1(\omega_1)\hat{S}^+_{yyo} & \dots & \Omega_p(\omega_1)\hat{S}^+_{yyo} \\ & \vdots & & \\ \Omega_0(\omega_{n_f})\hat{S}^+_{yyo} & \Omega_1(\omega_{n_f})\hat{S}^+_{yyo} & \dots & \Omega_p(\omega_{n_f})\hat{S}^+_{yyo} \end{bmatrix} \text{ for } o = 1,2,\dots,n_o \tag{42}$$

Finally, the scalar cost function can be calculated with the following matrix equation:

$$\varepsilon(\beta_o,\alpha) = \sum_{o=1}^{n_o} \mathrm{tr}\left\{E_o(\beta_o,\alpha)^H E_o(\beta_o,\alpha)\right\} = \sum_{o=1}^{n_o} \mathrm{tr}\left\{ \begin{bmatrix} \beta_o^T & \alpha^T \end{bmatrix} \begin{bmatrix} R_o & S_o \\ S_o^T & T_o \end{bmatrix} \begin{bmatrix} \beta_o \\ \alpha \end{bmatrix} \right\}$$
$$\text{with } R_o = \mathrm{Re}(X_o^H X_o),\ S_o = \mathrm{Re}(X_o^H Y_o),\ T_o = \mathrm{Re}(Y_o^H Y_o) \tag{43}$$

where tr{•} means the trace, or the sum of the elements in the main diagonal, of a matrix and Re(•) selects the real part of a complex number. The selection of the real part is due to the base assumption that the matrices to be determined, $B_r$ and $A_r$, are real-valued.

The minimum of the cost function is then determined by forcing its derivatives with respect to the unknowns (elements of the $B_r$ and $A_r$ matrices) to become zero:

$$\frac{\partial\varepsilon(\beta_o,\alpha)}{\partial\beta_o} = 2(R_o\beta_o + S_o\alpha) = 0 \quad \text{with} \quad o = 1,2,\dots,n_o$$
$$\frac{\partial\varepsilon(\beta_o,\alpha)}{\partial\alpha} = 2\sum_{o=1}^{n_o}(S_o^T\beta_o + T_o\alpha) = 0 \tag{44}$$

The first matrix equation with dimension $(p+1)$-by-$n_o$, contains the derivatives of the cost function with respect to all the elements stored in the matrices $\beta_o$. The second is a $n_o(p+1)$-by-$n_o$ matrix equation that contains the derivatives of the cost function with respect to all the elements organized in the $\alpha$ matrix.

With the aim of reducing the size of the system of equations to be solved, the unknowns $\beta_o$ can be eliminated:

$$2(R_o\beta_o + S_o\alpha) = 0 \Leftrightarrow \beta_o = -R_o^{-1}S_o\alpha \tag{45}$$

Consequently, matrix $\alpha$ can be obtained by solving the following reduced system of equations:

$$2\sum_{o=1}^{n_o}\left(T_o - S_o^T R_o^{-1} S_o\right)\alpha = 0 \Leftrightarrow M\alpha = 0 \tag{46}$$

where $M$ is $n_o(p+1)$-by-$n_o(p+1)$ matrix that can be calculated from the output half-spectrum matrix estimated from the measured time series.

In order to avoid the trivial solution of the previous equation ($\alpha$=0), a constraint has to be imposed. This can be done, for instance, by imposing that one of the $A_r$ matrices is equal to a non-zero constant value. This constraint also removes the parameters redundancy that exists in RMFD models (multiplying numerator and denominator with the same matrix yields different numerator and denominator polynomials, but the same transfer function or output spectrum matrix). The selection of the constraint has a huge impact on the quality of the results, as it will be illustrated afterwards in the processing of the data collected at the bridge. The described algorithm provides good results, if $A_0$ is forced to be an identity matrix.

Then, the resolution of the system of equations is elementary:

$$M\cdot\alpha = 0 \Leftrightarrow \left[\begin{array}{c|c} M_{aa} & M_{ab} \\ \hline M_{ba} & M_{bb} \end{array}\right] \cdot \begin{bmatrix} I \\ \hline A_1 \\ \vdots \\ A_p \end{bmatrix} = \begin{bmatrix} 0 \\ \hline 0 \\ \vdots \\ 0 \end{bmatrix} \Leftrightarrow$$
$$M_{bb}\cdot\alpha_b = -M_{ba} \Leftrightarrow \alpha_b = -M_{bb}^{-1}\cdot M_{ba} \tag{47}$$
$$\Rightarrow \alpha = \begin{bmatrix} I \\ -M_{bb}^{-1}\cdot M_{ba} \end{bmatrix}$$

$M_{ba}$ contains the first $n_o$ columns and the last $p\cdot n_o$ lines of $M$, $M_{bb}$ contains the last $pn_o$ columns and lines of $M$, and $\alpha_b$ contains the last $pn_o$ lines of $\alpha$.

Once the $A_r$ matrices have been determined, the $B_r$ matrices can be calculated using the relation between the $\alpha$ and $\beta_o$ matrices presented in Eq. (45). With this step, the identification problem is solved. It is now necessary to obtain the modal parameters of the identified model. This can be based on the transformation of the RMFD model fitted to the positive output spectrum matrix into an equivalent state-space model by the use of the expressions presented in Eq. (15). After this step, the identification follows the procedure already presented while describing the SSI-COV algorithm: determination of the eigenvalues and vectors of $A$ and subsequent calculation of the modal parameters. This model conversion has to be repeated as many times as the number of tried model orders, so that the modal parameters associated with different model

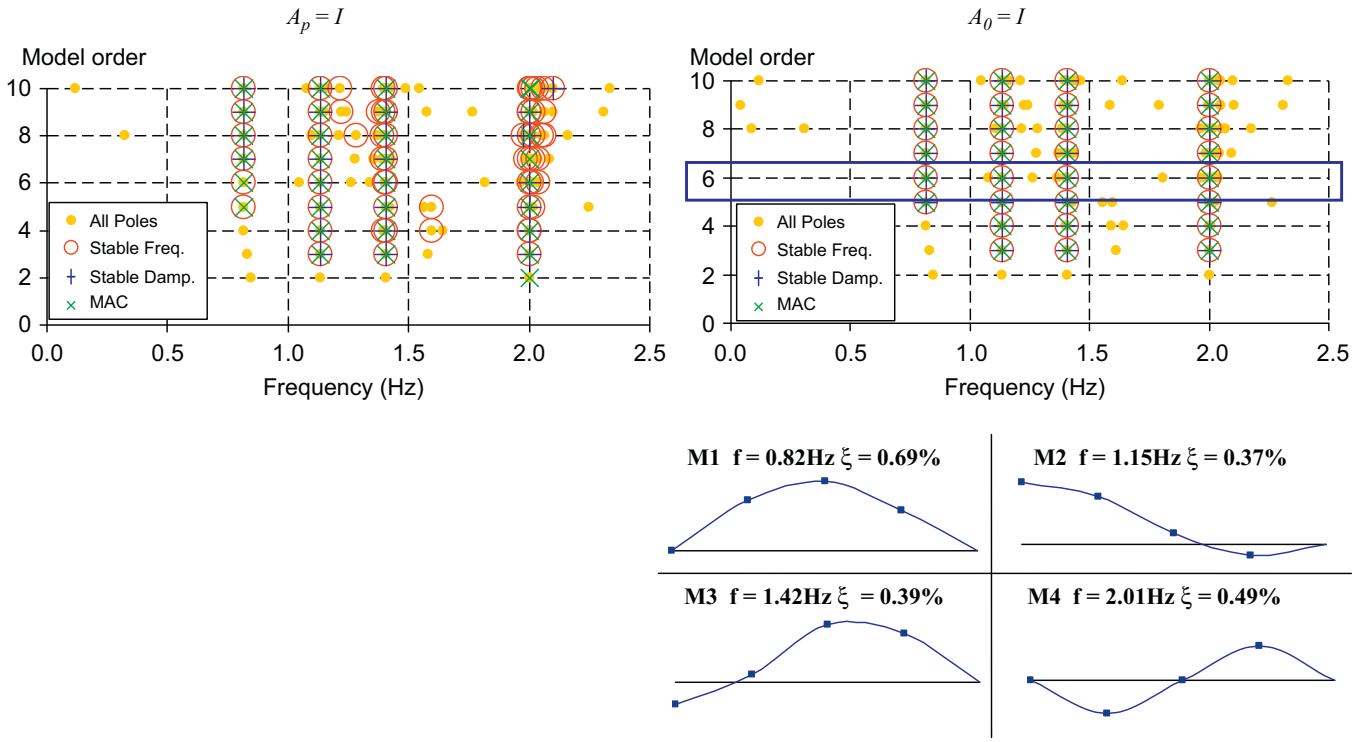


**Fig. 10.** p-LSCF method: stabilization diagram associated with two alternative constraints and selected mode estimates.

orders are represented in a stabilization diagram, which facilitates the selection of the physical modes of the tested structure.

The dataset collected at the Infante D. Henrique that was processed by the other two described methods was also analysed with the p-LSCF method. First of all, it was calculated a 4-by-4 matrix with the auto and cross half-spectra of the four acceleration time series presented in Fig. 3. These were obtained from the DFT of correlation functions of the outputs evaluated at 1024 positive time lags.

Afterwards, the $M$ matrix defined in Eq. (46) was constructed using the previously presented expressions and adopting for $p$ (the polynomial order) values between 2 and 10. A $\alpha$ matrix was determined for each of the 9 considered model orders using the equations presented in (47) and also imposing $A_p$ instead of $A_0$ to be an identity matrix. The obtained RMFD models were converted to state-space models from which mode estimates were extracted. These were organized in two stabilization diagrams, one for each considered constraint. The results presented in Fig. 10 show that the constraint defined in Eq. (47) provided an easier to interpret stabilization diagram, with four clear vertical alignments of stable poles. In fact, in the diagram presented at the left side, all mode estimates that are not associated with a physical mode present negative damping and so are easily separated from the estimates with physical meaning. The theoretical explanation for this very useful property of the algorithm is presented in [14]. The four mode estimates provided by polynomials with order 6 with the constrain $A_0$=$I$ and classified as stable are characterized at the bottom of Fig. 10.

The algorithm of the p-LSCF method can become more efficient if only some columns of the half-spectrum matrix are used. In [42] it is presented an algorithm based on reference outputs and on the identification of the modal parameters from the RMFD model matrices, instead of using its transformation to a state-space model. A methodology to compute confidence intervals for the estimates produced by this identification technique is presented by De Troyer et al. in [43]

## 5. Automated operational modal analysis

As ambient excitation is always present, the techniques used to analyse data collected during ambient vibration tests can be applied to continuously process time series acquired by a permanent installation of a set of accelerometers, as the one installed on the Infante D. Henrique Bridge. This permits to track the evolution of modal parameters over time. As structural deterioration or the occurrence of damages due to some extreme event, like an earthquake, implies a stiffness reduction and consequently a decrease of the natural frequencies, an accurate characterization of the variation of natural frequencies over time can be adopted to detect structural problems. This is the core idea behind vibration-based health monitoring systems.

However, the previously described techniques for identification of structural modal parameters require human intervention at some stages of analysis. Consequently, a lot of research has been developed with the goal of achieving

algorithms that can automatically extract accurate estimates of the structure modal parameters from its continuously recorded responses during normal operation conditions.

In the context of the monitoring project carried out at the Infante D. Henrique Bridge, it was used an innovative methodology for the automatic identification of modal parameters, using parametric identification methods, that is based on a hierarchical clustering algorithm. The method is suitable for the analysis of data produced by any parametric identification technique that provides estimates of natural frequencies, modal damping ratios and mode shapes for models of several orders. All the mode estimates provided by the identification algorithm are compared using a similarity measure that depends on the natural frequencies and on the MAC (Eq. (27)) between mode shape estimates. It groups the mode estimates associated with the same physical mode and permits the separation of the numerical or noisy estimates. All the details of this algorithm and also a review of other available methodologies are presented in [44]. Fig. 11 shows the time evolution of the modes analysed in the previous section (mode M1 to M4 characterized in Fig. 10). The estimates of the natural frequencies presented in the graphics resulted from the automatic processing of all the datasets collected from 13/09/2007 to 12/05/2010 with the cluster analysis applied to the outputs of the p-LSCF method. The influence of the annual temperature cycles on the natural frequencies is evident.

The processing of data collected by dynamic monitoring systems with the aim of identifying structural deficiencies comprehends not only automatic identification of modal parameters, but also elimination of the environmental and operational effects on natural frequencies. As the identification of very small structural changes is aimed to permit the detection of damages in an early phase of development, the minute effects of for instance the temperature or the traffic intensity over a bridge on the natural frequencies have to be minimized. Therefore, monitoring software based on OMA has to include three components: (i) automatic identification of modal parameters, (ii) elimination of the environmental and operational effects on modal parameters, (iii) calculation of an index able to flag relevant frequency shifts. These steps are illustrated in Fig. 12 using results from the Infante D. Henrique Bridge. The algorithm for automated operational modal analysis, in continuous operation for more than 2 years, has permitted the characterization of the time evolution of the bridge first 12 natural frequencies. The algorithms implemented to calculate an index able to detect structural anomalies prove to be efficient on identification of numerically simulated damages. All the details of this analysis are described in [45]. In [46], it is presented another application where the ability of a vibration-based monitoring systems to detect damages was proven, in this case with the introduction of real damages in the bridge under study.

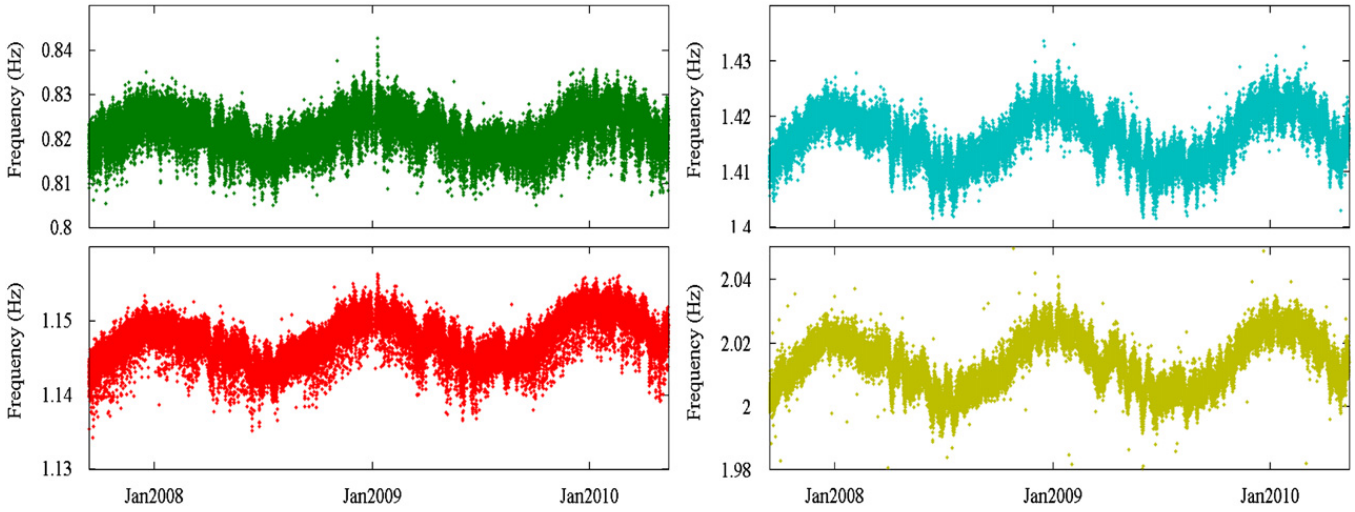


**Fig. 11.** Time evolution of the natural frequencies of the first four vertical bending modes.

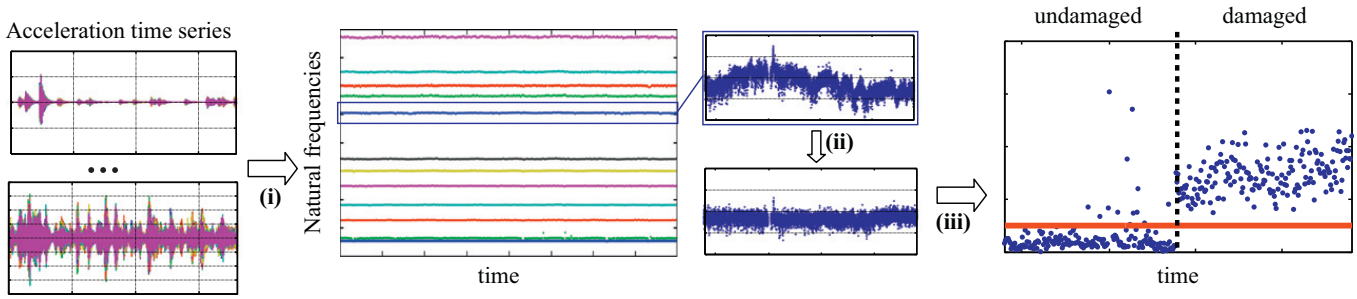


**Fig. 12.** Main processing steps of a vibration-based health monitoring system.

## 6. Conclusions

This tutorial paper presents an introduction to the use of operational modal analysis. A brief review of the theoretical background of alternative models of dynamic systems is followed by the description of three of the most powerful algorithms for the identification of modal parameters from structural responses to ambient excitation. In order to make the exposition more didactic, the most important mathematical steps were illustrated with the processing of data collected in an arch bridge. At the end, it was stressed the usefulness of operational modal analysis in the context of Structural Health Monitoring systems.

Some of the most important references that permit a further broadening and deepening of the readers knowledge about the theoretical aspects involved in operational modal analysis have already been mentioned in the introduction of Section 4. Now, it is relevant to point out some works with recent and interesting applications. In [47], it is described the ambient vibration test of the Humber Bridge, the largest suspension bridge in the United Kingdom; Siringoringo and Fujino [48] describe the processing of a database collected in a suspension bridge in Japan (Hakucho Bridge); in [49] several relevant applications on bridges and other special structures are presented; in [50], it is demonstrated the usefulness of ambient vibration tests in the context of the implementation of vibration control devices; Pakzad and Fences [51] present the results obtained with an ambient vibration test performed on the Golden Gate Bridge with wireless sensors; Carne and James III [52] describe the use of OMA in wind turbines testing; reference [53] characterizes the monitoring of historical masonry structures, taking profit from OMA.

The applications on large civil engineering structures described in the previously mentioned papers prove that operational modal analysis has already achieved significant maturity. However, there are also some limitations, such as the uncertainty of the modal damping estimates [54], which justify the need for further research to make this experimental tool even more powerful and useful.

## References


[1] D.J. Ewins, Modal Testing: Theory and Practice, Research Studies Press, UK, 2000.
[2] W. Heylen, S. Lammens, P. Sas, Modal Analysis Theory and Testing, KULeuven, Belgium, 2007.
[3] N. Maia, J. Silva, Theoretical and Experimental Modal Analysis, Research Studies Press Ltd., 1997.
[4] Á. Cunha, E. Caetano, Experimental modal analysis of civil engineering structures, Sound and Vibration 6 (40) (2006) 12–20.
[5] E. Parloo, P. Verboven, P. Guillaume, M.V. Overmeire, Sensitivity-based operational mode shape normalization, Mechanical Systems and Signal Processing 16 (5) (2002) 757–767.
[6] R. Brincker, P.H. Kirkegaard, Special issue on operational modal analysis, Mechanical Systems and Signal Processing 24 (5) (2009) 1209–1212.
[7] A. Adão da Fonseca, F. Millanes Mato, Infante Henrique Bridge over the River Douro, Porto, Portugal, Structural Engineering International 15 (2) (2005) 85–87.
[8] F. Magalhães, Á. Cunha, E. Caetano, Dynamic monitoring of a long span arch bridge, Engineering Structures 30 (11) (2008) 3034–3044.
[9] M.I. Friswell, J.E. Mottershead, Finite Element Model Updating in Structural Dynamics, Kluwer Academic Publishers, 1995.
[10] J.-N. Juang, Applied System Identification, Prentice Hall, Englewood Cliffs, NJ, USA, 1994.
[11] B. Peeters, System identification and damage detection in civil engineering, Ph.D. Thesis, Katholieke Universiteit, Leuven, Belgium, 2000.
[12] P. Van Overschee, B. De Moor, Subspace Identification for Linear Systems, Kluwer Academic Publishers, Leuven, Belgium, 1996.
[13] B. Cauberghe, Applied frequency-domain system identification in the field of experimental and operational modal analysis, Ph.D. Thesis, Vrije Universiteit, Brussel, Belgium, 2004.
[14] E. Reynders, System identification and modal analysis in structural mechanics, Ph.D. Thesis, Katholieke Universiteit, Leuven, Belgium, 2009.
[15] L. Ljung, System Identification: Theory for the User, Prentice-Hall, New Jersey, 1999.
[16] V.R. MacLamore, G.C. Hart, I.R. Stubbs, Ambient vibration of two suspension bridges, Journal of the Structural Division, ASCE 97 (ST10) (1971) 2567–2582.
[17] P., Guillaume, L. Hermans, H. Van der Auweraer, Maximum likelihood identification of modal parameters from operational data, in: Proceedings of IMAC 17, International Modal Analysis Conference, Kissimmee, FL, USA, 1999.
[18] C. Devriendt, P. Guillaume, The use of transmissibility measurements in output-only modal analysis, Mechanical Systems and Signal Processing 21 (7) (2007) 2689–2696.
[19] J. Bendat, A. Piersol, Engineering Applications of Correlation and Spectral Analysis, John Wiley & Sons, USA, 1980.
[20] J.-N. Juang, R.S. Pappa, An eigensystem realization algorithm for modal parameter identification and model reduction, Journal of Guidance, Control, and Dynamics 8 (5) (1985) 620–627.
[21] G.H. James, T.G. Carne, J.P. Lauffer, A.R. Nard, Modal testing using natural excitation, in: Proceedings of IMAC 10, International Modal Analysis Conference, San Diego, USA, 1992.
[22] P. Andersen, Identification of civil engineering structures using vector ARMA models, Ph.D. Thesis, Aalborg University, Denmark, 1997.
[23] A.V. Oppenheim, R.W. Schafer, Digital Signal Processing, Prentice-Hall, 1975.
[24] P.D. Welch, The use of fast Fourier transform for the estimation of power spectra: a method based on time averaging over short modified periodograms, IEEE Transaction on Audio and Electro-Acoustics AU-15 (1967) 2.
[25] R. Brincker, L. Zhang, P. Andersen, Modal identification from ambient responses using frequency domain decomposition, in Proceedings of the IMAC 18, International Modal Analysis Conference, San Antonio, USA, 2000.
[26] M. Prevosto, Algorithmes D'Identification des Caractéristiques Vibratoires de Structures Mecaniques Complexes, Ph.D. Thesis, Université de Rennes I, France, 1982.
[27] M.R. Corrêa, A.C. Costa, Dinamic tests of the bridge over the Arade River, in: J.A. Fernandes, L.O. Santos (Eds.), Cable-stayed Bridges of Guadiana and Arade, Book, LNEC, 1992 (in Portuguese).
[28] C.Y. Shih, Y.G. Tsuei, R.J. Allemang, D.L. Brown, Complex mode indicator function and its application to spatial domain parameter estimation, Mechanical Systems and Signal Processing 2 (4) (1988) 367–377.
[29] R.J. Allemang, D.L. Brown, A correlation coefficient for modal vector analysis, in: Proceedings of the IMAC 1, International Modal Analysis Conference, Orlando, FL, USA, 1982.
[30] R.W. Clough, J. Penzien, Dynamics of Structures, McGraw-Hill, 1993.
[31] R., Brincker, C. Ventura, P. Andersen, Damping estimation by frequency domain decomposition, in Proceedings of the IMAC 19, International Modal Analysis Conference, Kissimmee, FL, USA, 2001.

[32] N.-J. Jacobsen, P. Andersen, R. Brincker, Applications of frequency domain curve-fitting in the EFDD technique, in: Proceedings of IMAC 26, International Modal Analysis Conference, Orlando, FL, USA, 2008.
[33] F. Magalhães, E. Caetano, Á. Cunha, Operational modal analysis and finite element model correlation of the Braga Stadium suspended roof, Engineering Structures 30 (6) (2008) 1688–1698.
[34] J. Rodrigues, R. Brincker, P. Andersen, Improvement of frequency domain output-only modal identification from the application of the random decrement technique, in: Proceedings of the IMAC 22, International Modal Analysis Conference, Dearborn, USA, 2004.
[35] L. Zhang, T. Wang, Y. Tamura, A frequency-spatial domain decomposition (FSDD) method for operational modal analysis, Mechanical Systems and Signal Processing 24 (5) (2009) 1227–1239.
[36] S.Y. Kung, A new identification and model reduction algorithm via singular value decomposition, in Proceedings of the 12th Asilomar Conference on Circuits, Systems and Computers, USA, 1978.
[37] MatLab2000, Using MATLAB Version 6, The MathWorks.
[38] B. Peeters, G. De Roeck, Reference-based stochastic subspace identification for output-only modal analysis, Mechanical Systems and Signal Processing 13 (6) (1999) 855–878.
[39] E. Reynders, R. Pintelon, G. De Roeck, Uncertainty bounds on modal parameters obtained from stochastic subspace identification, Mechanical Systems and Signal Processing 22 (4) (2008) 948–969.
[40] P. Guillaume, P. Verboven, S. Vanlanduit, H. Van der Auweraer, B. Peeters, A poly-reference implementation of the least-squares complex frequency-domain estimator, in: Proceedings of the IMAC 21, International Modal Analysis Conference, Kissimmee, FL, USA, 2003.
[41] B. Peeters, H. Van Der Auweraer, P. Guillaume, J. Leuridan, The PolyMAX frequency-domain method: a new standard for modal parameters estimation?, Shock and Vibration 11 (2004) 395–409.
[42] B. Peeters, H. Van Der Auweraer, PolyMax: a revolution in operational modal analysis, in: Proceedings of the IOMAC, International Operational Modal Analysis Conference, Copenhagen, Denmark, 2005.
[43] T. De Troyer, P. Guillaume, R. Pintelon, S. Vanlanduit, Fast calculation of confidence intervals on parameter estimates of least-squares frequency-domain estimators, Mechanical Systems and Signal Processing 23 (2) (2009) 261–273.
[44] F. Magalhães, Á. Cunha, E. Caetano, Online automatic identification of the modal parameters of a long span arch bridge, Mechanical Systems and Signal Processing 23 (2) (2009) 316–329.
[45] F. Magalhães, Operational modal analysis for testing and monitoring of bridges and special structures, Ph.D. Thesis, Faculty of Engineering of the University of Porto, 2010.
[46] B. Peeters, G. De Roeck, One-year monitoring of the Z24-Bridge: environmental effects versus damage events, Earthquake Engineering and Structural Dynamics 30 (2) (2001) 149–171.
[47] J.M.W. Brownjohn, F. Magalhães, E. Caetano, Á. Cunha, Ambient vibration re-testing and operational modal analysis of the Humber Bridge, Engineering Structures (2010).
[48] D.M. Siringoringo, Y. Fujino, System identification of a suspension bridge from ambient vibration response, Engineering Structures 30 (2) (2008) 462–477.
[49] Á. Cunha, E. Caetano, F. Magalhães, Output-only dynamic testing of bridges and special structures, Structural Concrete (Fib) 8 (2) (2007) 67–85.
[50] E. Caetano, Á. Cunha, F. Magalhães, C. Moutinho, Studies for controlling human-induced vibration of the Pedro e Inês footbridge, Portugal. Part 1: Assessment of dynamic behaviour, Engineering Structures 32 (4) (2010) 1069–1081.
[51] S.N. Pakzad, G.L. Fences, Statistical analysis of vibration modes of a suspension bridge using spatially dense wireless sensor network, Journal of Structural Engineering 135 (7) (2009) 863–872.
[52] T.G. Carne, G.H. James III, The inception of OMA in the development of modal testing technology for wind turbines, Mechanical Systems and Signal Processing 24 (5) (2009) 1213–1226.
[53] L.F. Ramos, L. Marques, P.B. Lorenço, Guido De Roeck, A. Campos Costa, J. Roque, Monitoring historical masonry structures with operational modal analysis: two case studies, Mechanical Systems and Signal Processing 24 (5) (2009) 1291–1305.
[54] F. Magalhães, Á. Cunha, E. Caetano, R. Brincker, Damping estimation using free decays and ambient vibration tests, Mechanical Systems and Signal Processing 24 (5) (2009) 1274–1290.